Optical frequency combs generated by acousto-optic frequency-shifting loops

Vicente Durán, Hugues Guillet de Chatellus, Côme Schnébelin, Kanagaraj Nithyanandan, Léo Djevarhidjian, Juan Clement, Carlos R. Fernández-Pousa, *Senior Member, IEEE*

***Abstract*— A recirculating loop that includes an acousto-optic frequency shifter (AOFS) constitutes a versatile procedure to generate an optical frequency comb (OFC) from a continuous wave (cw) laser. This scheme, implementable with conventional fiber equipment, is capable of producing spectra composed of at least hundreds of coherent lines using a single-stage system. In this paper, we summarize the method to generate these acousto-optic frequency combs and briefly describe a simple model to optimize their performance. We also overview their main reported applications, paying special attention to those based on the peculiarities exhibited by the optical field at the output of the fiber loop.**

***Index Terms*— Acousto-optic devices, fiber loops, high-resolution spectroscopy, laser raging, optical frequency combs, photonic signal processing.**

I. Introduction

A simple and robust manner of generating an OFC is based on the feeding of one or several electro-optic (EO) modulators by a single continuous-wave laser [1-3]. Unlike approaches that employ laser cavities, EO frequency combs offer a line spacing that can be easily tuned over orders of magnitude, from hundreds of MHz to tens of GHz [3]. In addition, this type of combs has aroused great interest to perform dual-comb spectroscopy (DCS), since two OFCs with different line spacing can be generated from the same laser line, thus exhibiting a high degree of mutual coherence by construction [4-6]. Despite these advantages, the generated combs typically feature a relatively low number of optical lines (<100), even when several EO modulators are placed in cascade. This limitation can be overcome, by instance, through external nonlinear broadening [7,8]. Alternatively, OFCs with thousands of lines and a very small line spacing (<10 MHz) can be produced by driving an EO modulator with trains of linearly chirped waveforms or optimized bit sequences [9,10]. All these approaches can be combined to generate broadband ultra-dense combs, but at the cost of employing a progressively more complex multi-stage comb generator [11].

Another easily implementable manner of generating OFCs from a cw laser, although considerably less exploited, is based on the use of an AOFS inserted in a recirculating loop [12-14]. Outstandingly, this simple scheme, to be reviewed in the present paper, produces spectra containing 100s or even >1000 lines without resorting to nonlinear broadening or optimized driving schemes, even though the line spacing is typically limited to values below 1 GHz. When a larger separation between lines is intended, the AO frequency shifter can be replaced by an EO modulator [15-17], but in that case the total number of lines generated by the loop usually ranges from a few tens to one hundred. In addition, the use of a single sideband EO shifter produces an unavoidable third harmonic, leading to cross-talk effects between the generated lines [17]. For that reason, when a relatively small line spacing is required, AO frequency shifters offer extinction ratios exceeding 50 dB, better performance in terms of efficiency and number of generated lines, and some remarkable features for applications in the time domain [18]. Indeed, these features have been exploited for the generation of optical/RF signals in laser ranging and sensing [13,14,19,20], as well as for the implementation of real-time signal processors [21,22].

II. Comb generation principle

Figure 1(a) shows a typical scheme of an AO frequency-shifting loop (AO-FSL). It contains an AO frequency shifter (AOFS), an erbium-doped fiber amplifier (EDFA) and a tunable bandpass filter (TBPF). An input coupler is used to feed the loop with a cw laser of frequency f_0 (linewidth<1 kHz), while an output coupler extracts a fraction of the field traveling in the FSL. Every round-trip time τ_c inside the loop, the frequency of the light is shifted by a quantity given by the frequency f_s of the signal driving the AOFS. The result of this process is the generation of a comb with a line spacing equal to f_s, regardless of the value of τ_c, which is set by the optical length of the loop. The parameter f_s typically takes values of tens or hundreds of megahertz. However, the line spacing can be reduced to the megahertz or sub-megahertz level by using two AO modulators that introduce frequency shifts with opposite signs [23]. The frequency f_n of the n-th tooth is given by $f_n = f_0 + nf_s$ ($n = 0, \ldots, N–1$), being N the number of lines, see Fig. 1(b). The generation of a coherent comb requires the use of a narrow-linewidth laser, whose coherence time must largely exceed $\tau_c N$. The EDFA compensates for the losses in the loop, while the role of the TBPF is two-fold: (i) it controls the total number of lines, and (ii) limits the spectral bandwidth of the amplified spontaneous emission (ASE) originated in the EDFA.

This work was supported by Ministerio de Ciencia, Innovación y Universidades, Agencia Estatal de Investigación, Spain; and European Union (FEDER) (RYC-2017-23668, TEC2017-89688-P and RTI2018-097957-B-C32), and by Agence Nationale de la Recherche (ANR-14-CE32-0022).

H.G.C., C.S., K. N., and L.D. are with Univ. Grenoble Alpes, CNRS, LIPhy, 38000 Grenoble, France. J.C. and C.R.F-P. are with Engineering Research Center (13E), Dep. of Communications Engineering, Univ. Miguel Hernandez, 03202 Elche, Spain. V.D. is with GROC-UJI, Dep. of Physics, Universitat Jaume I, Castellón, 12071 Spain (e-mail: vduran@uji.es).

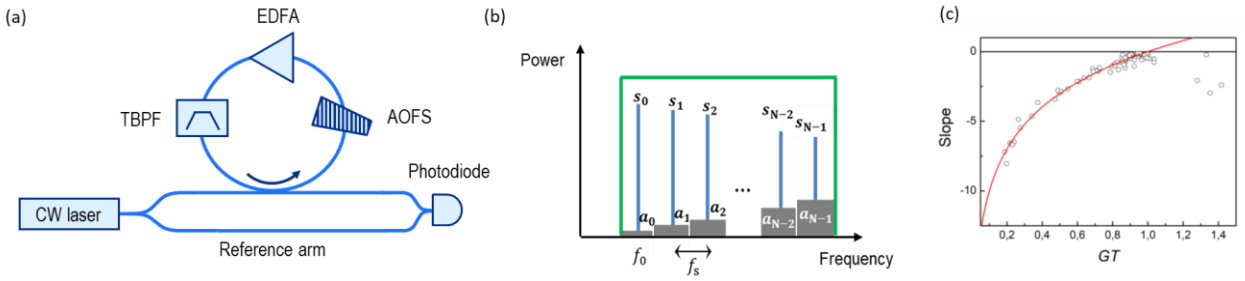

Fig. 1. (a) Sketch of an AO-FSL. By mixing with the cw laser (reference arm) it is possible to perform self-heterodyne interferometry. (b) Scheme of the one-sided comb spectrum, composed of N lines, originated by an AO-FSL. (c) Slope of the comb envelope (in log scale) as a function of $G \times T$ [18]. The experimental points were obtained for about 60 sets of loop parameters, by varying the pump current of the EDFA, T, and s_0.

III. Power Spectrum

A simple model for predicting the power spectrum generated by an AO-FSL can be developed on the basis of a few assumptions: (i) the system is considered to be in the steady state, (ii) the gain is the same for all the comb teeth and (iii) the optical bandpass filter in the loop has an ideal flat-top transmission function. We define s_0 as the power of the seed laser injected in the FSL. The total number of teeth is in principle set by the bandwidth of the optical TBPF. Our model is based on the fact that the power s_n of the n-th tooth is equal to the product of the power s_{n-1} corresponding to the $(n-1)$-th tooth and the *net* power transmission coefficient of the loop. We define this coefficient as the product $G \times T$, where G is the amplification factor introduced by the gain medium, and T is the power transmission coefficient of the loop excluding the amplifier, so that $s_n = (G \times T)^n s_0$ .This expression evidences an exponential variation of the comb envelope, which is an increasing (decreasing) function when $G \times T > 1$ ($G \times T$<1). We now define a_n as the ASE power in a frequency band of width f_s, centered around f_n, which is equal to the product of a_{n-1} and the net power transmission coefficient of the round-trip loop, plus an additional term a_0 corresponding to the excess of ASE power emitted by the amplifier. This second term can be written as $a_0 = 2n_{sp}h\nu\,(G-1)f_s$, where $n_{sp} > 1$ is the spontaneous emission factor (directly related to the noise figure *NF* of the amplifier), and h and ν are respectively the Planck's constant and the central frequency of the photons [24]. Here, ν can be approximate by f_0 for all the comb teeth, since the spectrum bandwidth is orders of magnitude lower than the laser frequency. Therefore, the resulting ASE power in the spectral band around f_n is $a_n = G \times T \times a_{n-1} + a_0$, and so

$$a_n = \sum_{k=0}^{n}(G \times T)^k a_0 = \frac{1-(G\times T)^{n+1}}{1-G\times T}\,a_0, \qquad (1)$$

being $a_0 = 2n_{sp}hf_0(G-1)f_s$. Concerning the amplification factor, it is given by [24]

$$G = \exp\left(\frac{g_{ss}}{1+P_{tot}/P_{sat}}\right), \qquad (2)$$

where g_{ss} is the (dimensionless) small signal gain, $P_{tot} = \sum_n(s_n + a_n)$ is the total power, and P_{sat} is the saturation power of the amplifier. From g_{ss}, we can also define $G_{ss} = \exp(g_{ss})$ as the small signal amplification factor of the amplifier.

The above set of equations is sufficient to determine the spectrum at the output of an AO-FSL, as well as to analyze the influence of various experimental parameters, such as N, f_s, s_0, NF, G_{ss} and T. Fig. 1(c), for instance, reveals that the slope of the comb critically depends on the product $G \times T$. The data shown in this figure, reported and explained in [18], are retrieved from self-heterodyne measurements of an AO-OFC with a line spacing of 50 kHz. As a general design rule, using amplifiers with small *NF* and reducing the losses of the loop have a positive influence on the comb flatness. By means of a proper optimization, it is possible to produce a relatively flat comb with >1000 lines, as is shown in Fig. 2 [14,19].

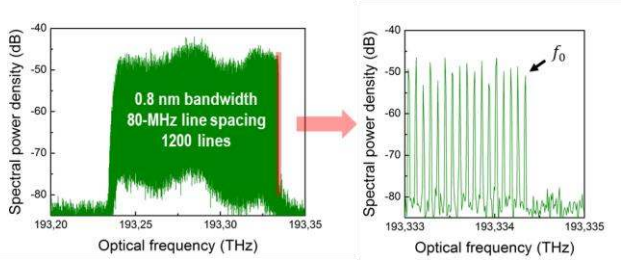

Fig. 2. Experimental 100 GHz-bandwidth OFC generated from an AO-FSL, measured with a high-resolution optical spectrum analyzer [19].

IV. FSL Optical Field

The frequency combs generated by AO-FSLs provide a variety of periodic optical fields, which are ultimately determined by the relative spectral phases between different comb lines. We assume that dispersive effects due to the propagation inside the fiber loop can be neglected. Under this approximation, and writing the light field injected into an unidirectional FSL as $E(t) = E_0\exp(i2\pi f_0 t)$, the loop's output can be expressed as a single-sided sum of spectral lines, $E_{FSL}(t) = \sum_{n=0}^{N-1} E_n \exp[i2\pi(f_0 + nf_s)t]$, each generated by the n-th pass of the injected field through the loop. The spectral amplitudes are then given by [19,25]:

$$E_n = E_0 g_n e^{-i2\pi[nf_0\tau_c + n(n+1)f_s\tau_c/2]}\,. \qquad (3)$$

In this equation, g_n characterize the comb's envelope, so that the output spectral power is $s_n = |E_0|^2 g_n^2$. The spectral phase in Eq. (3) exhibits a linear term in n, which originates a delay $\tau = f_0\tau_c/f_s + \tau_c/2$ linearly dependent on the input frequency f_0, together with a second term quadratic in n, which can be

interpreted as equivalent to that induced by linear dispersion.

The resulting optical fields can be classified according to the theory of temporal Talbot effect [26], depending on the product $\phi = f_s\tau_c$, which is easily tunable through the driving frequency f_s. If ϕ is an integer p, the output is simply a sequence of transform-limited pulses at a rate f_s (integer Talbot effect). In turn, when ϕ is equal to an irreducible fraction of the form p/q, the output period is composed of q transform-limited pulses with equal energy and equally spaced within the period (fractional Talbot effect) and with relative phases given by a Gauss phase sequence [27,28]. Laser oscillation at fractional Talbot conditions, where qf_s equals the p-th harmonic of the loop's free spectral range $1/\tau_c$, has been demonstrated (see, for instance, the dye laser in [29]). However, the non-oscillating loop permits a wider range of operation conditions in terms of the frequency shift per round trip, leading to trains of dispersed pulses. Indeed, if f_s is just slightly detuned by an amount δf_T from a certain integer or fractional Talbot condition, the generated pulses are stretched by a controllable group velocity dispersion $D = \tau_c\delta f_T/(2\pi f_s^2)$ [19].

An example of the quadratic spectral phase acquired in this situation is shown in Fig. 3. Strikingly, the corresponding amount of linear dispersion is equivalent to that introduced by an extremely long optical dispersive line, and therefore the wave reaches the time-domain far-field region. The AO-FSL amplitude is then a scaled replica of the optical spectrum and its phase is linearly chirped [19]. In Fig. 4, we present the heterodyne signal, or in-phase component of the wave field, corresponding to a small detuning in f_s of the 1/12 Talbot condition, and in Fig. 5 it can be observed a dispersed integer Talbot field and its instantaneous frequency, showing a chirp factor of ~2 GHz/ns.

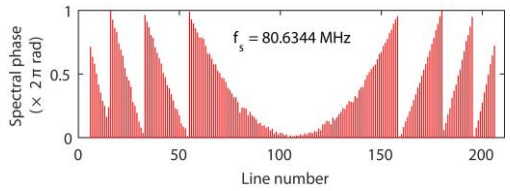

Fig. 3. Wrapped spectral phase for 200 spectral lines, covering an optical bandwidth of 16 GHz. The line spacing is detuned from the Talbot condition 5 kHz. This curve is retrieved through a DCS measurement using a second frequency comb with a flat spectral phase (i.e., set at the Talbot condition), see details in [25]. The spectral phase observed here is equivalent to the dispersion introduced by about 1000 km of a conventional single-mode fiber.

V. Applications

In the time domain, the temporal Talbot effect observed in AO frequency combs has been exploited for generating trains of pulses with reconfigurable repetition rates [13,29]. Indeed, an AO-FSL can be employed to achieve a wide control, over several orders of magnitude, of the line spacing of a frequency comb [14]. On the other hand, FSLs have been utilized to create broadband chirped waveforms [19] and also to perform real-time Fourier transformation (RTFT) [21]. In the latter case, the RTFT is obtained due to the frequency-to-time mapping implemented by the linear relationship between input optical frequencies and overall delays, as was described in the previous section. This scheme has demonstrated to overcome frequency-resolution limitations of dispersion-based RTFT schemes, achieving a resolution of ≃30 kHz and a time–bandwidth product exceeding 400 with minimum latency time. This concept has been extended to the generation of fractional Fourier transforms [22] and arbitrary electrical waveforms [30].

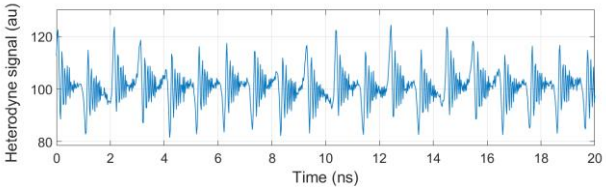

Fig. 4. Self-heterodyne signal of the AO-FSL in [20] corresponding to a small detuning of the 1/12 Talbot condition. The periodic output, of period 12.5 ns, is composed of 12 dispersed pulses, each with a different phase given by a Gauss perfect phase sequence.

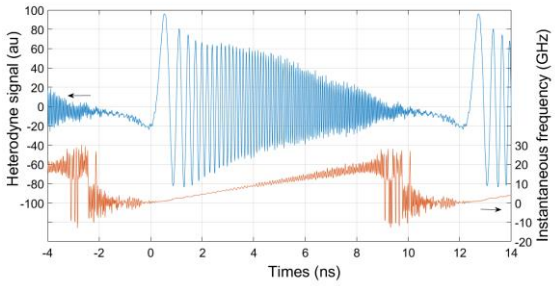

Fig. 5. Self-heterodyne signal (blue, left axis) and instantaneous frequency (orange, right axis) of the output of an AO-FSL tuned to f_s = 82.018 MHz, which represents an increase of 43 kHz with respect to the p = 6 integer Talbot condition for that loop.

In the frequency domain, AO-FSLs have proved to be a simple and compact comb platform to conduct multi-heterodyne interferometry. By means of a single acousto-optic frequency comb containing two AO shifters, it has been carried out self-heterodyne interferometry with sub-MHz point spacing (500 kHz). By increasing the line spacing up to tens of MHz (75-80 MHz), two mutually coherent AO-FSLs have been employed to perform DCS in the near-infrared region [23]. In a further development, this system has been simplified using a bidirectional FSL, capable of producing two counter-propagating OFCs with different line spacing [25]. Apart of avoiding duplications, this scheme has demonstrated to reach acquisition times > 0.1 s without resorting to stabilization feedback loops, thanks to the common-noise rejection provided by the bidirectional configuration. A comprehensive analysis of the attainable signal-to-noise ratio, as well its evolution with the line number, can also be found in [25].

AO-FSL have also been employed to perform laser ranging using digital pulse compression [20]. This application exploits the fact that the self-heterodyne signal of the one-sided FSL spectrum allows the retrieval of the full, complex electric field by use of the Hilbert transform, without the need of I/Q receivers. Then, the field at the output of an optical circuit can be digitally cross-correlated with the FSL input field, showing a series of peaks located at each of the reflector's position. These peaks are described by its periodic autocorrelation $R(u)$, which, according to the Wiener-Kintchine theorem, is the Fourier transform of the power spectrum:

$$R(u) = \int_0^{\frac{1}{f_s}} dt\, E^*_{FSL}(t) E_{FSL}(t+u) = \sum_{n\geq 0} s_n e^{-i2\pi n f_s u}. \quad (4)$$

An example of the concept in a meter scale interferometer is given in Fig. 6. As is described in detail in [20], the distance resolution (4 mm) is only limited here by the available detection bandwidth (20 GHz).

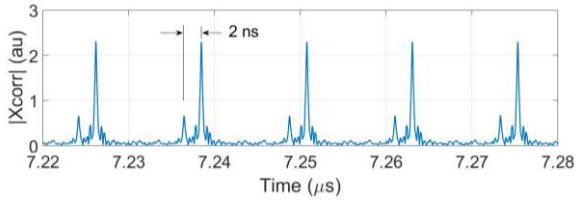

Fig. 6. Digital cross-correlation between the optical field at the output of a composite fiber-free space interferometer and the reference field, obtained by blocking the free space arm [20]. The separation between cross-correlation peaks, which represent the positions of the interferometer's mirrors, corresponds to a single-pass distance of 30 cm in free space.

VI. Conclusions

AO-FSLs represent a simple, cost-effective and versatile means of producing frequency combs from a cw laser, with a line spacing that can range from less than 1 MHz to ~100 MHz. Through a proper optimization of the loop parameters, the total number of usable spectral lines can reach values above 1000, covering an optical bandwidth that can range from less than 1 GHz to ~100 GHz. This spectral coverage could be dramatically increased by the design of multi-stage generators that combine different comb approaches [11]. It should be noted, however, that all the above achievements require stable loop configurations over relatively long time scales. A detailed analysis of the noise properties of AO-FSLs, analogous to some developed for EO-FSLs [16,17], is under investigation and the subject of further publications. Despite that, AO frequency combs have emerged as a compact solution for the agile generation of optical fields in a variety of applications, including spectroscopy, signal processing, and laser ranging.

References

[1] T. Kobayashi, H. Yao, K. Amano, Y. Fukushima, A. Morimoto, and T. Sueta, "Optical pulse compression using high-frequency electrooptic phase modulation," IEEE J. Quantum Electron., vol. 24, no. 2, pp. 382–387, 1988.

[2] H. Murata, A. Morimoto, T. Kobayashi, and S. Yamamoto, "Optical pulse generation by electrooptic-modulation method and its application to integrated ultrashort pulse generators," IEEE J. Sel. Top. Quantum Electron., vol. 6, no. 6, pp. 1325–1331, 2000.

[3] V. Torres-Company and A. M. Weiner, "Optical frequency comb technology for ultra-broadband radio-frequency photonics," Laser Photon. Rev., vol. 8, no. 3, pp. 368–393, May 2014.

[4] D. A. Long et al., "Multiheterodyne spectroscopy with optical frequency combs generated from a continuous-wave laser," Opt. Lett., vol. 39, no. 9, pp. 2688–2690, 2014.

[5] P. Martín-Mateos, B. Jerez, and P. Acedo, "Dual electro-optic optical frequency combs for multiheterodyne molecular dispersion spectroscopy," Opt. Express, vol. 23, no. 16, pp. 21149–21158, 2015.

[6] V. Durán, S. Tainta, and V. Torres-Company, "Ultrafast electrooptic dual-comb interferometry," Opt. Express, vol. 23, no. 23, pp. 30557–30569, 2015.

[7] G. Millot et al., "Frequency-agile dual-comb spectroscopy," Nat. Photonics, vol. 10, no. May, pp. 27–30, 2016.

[8] V. Durán, P. A. Andrekson, and V. Torres-Company, "Electro-optic dual-comb interferometry over 40 nm bandwidth," Opt. Lett., vol. 41, no. 18, pp. 4190–4193, 2016.

[9] D. A. Long, A. J. Fleisher, D. F. Plusquellic, and J. T. Hodges, "Multiplexed sub-Doppler spectroscopy with an optical frequency comb," Phys. Rev. A, vol. 061801(R), 2016.

[10] L. Yan, X. Zou, X. Yan, J. Azaña, and W. Pan, "Fully digital programmable optical frequency comb generation and application," Opt. Lett., vol. 43, no. 2, pp. 283–286, 2018.

[11] B. Xu, X. Fan, S. Wang, and Z. He, "Broadband and high-resolution electro-optic dual-comb interferometer with frequency agility," Opt. Express, vol. 27, no. 6, pp. 9266–9275, 2019.

[12] P. Coppin and T. G. Hodgkinson, "Novel optical frequency comb synthesis using optical feedback," Electron. Lett., vol. 26, no. 1, pp. 28–30, 1990.

[13] H. Guillet de Chatellus, E. Lacot, W. Glastre, O. Jacquin, and O. Hugon, "Theory of Talbot lasers," Phys. Rev. A - At. Mol. Opt. Phys., vol. 88, no. 3, p. 033828, 2013.

[14] H. Guillet de Chatellus, L. Romero Cortés, and J. Azaña, "Arbitrary energy-preserving control of the line spacing of an optical frequency comb over six orders of magnitude through self-imaging," Opt. Express, vol. 26, no. 16, pp. 21069–21085, 2018.

[15] K.-P. Ho and J. M. Kahn, "Optical Frequency Comb Generator Using Phase Modulation in Amplified Circulating Loop," *IEEE Photonics Technol. Lett.*, vol. 5, no. 6, pp. 721–725, 1993.

[16] P. Shen, N. J. Gomes, S. Member, P. A. Davies, P. G. Huggard, and B. N. Ellison, "Analysis and Demonstration of a Fast Tunable Fiber-Ring-Based Optical Frequency Comb Generator," *J. Light. Technol.*, vol. 25, no. 11, pp. 3257–3264, 2007.

[17] J. Li, X. Li, X. Zhang, F. Tian, and L. Xi, "Analysis of the stability and optimizing operation of the single-side-band modulator based on re-circulating frequency shifter used for the T-bit / s optical communication transmission," *Opt. Express*, vol. 18, no. 17, pp. 17597–17609, 2010.

[18] N. Kanagaraj, L. Djevarhidjian, V. Duran, C. Schnébelin, and H. G. de Chatellus, "Optimization of acousto-optic optical frequency combs," Opt. Express, vol. 27, no. 10, p. 14842, 2019.

[19] H. G. De Chatellus, L. Romero Cortés, C. Schnébelin, M. Burla, and J. Azaña, "Reconfigurable photonic generation of broadband chirped waveforms using a single CW laser and low-frequency electronics," Nat. Commun., vol. 9, p. 2438, 2018.

[20] J. Clement, C. Schnébelin, H. G. de Chatellus, and C. R. Fernández-Pousa, "Laser ranging using coherent pulse compression with frequency shifting loops," Opt. Express, vol. 27, no. 9, pp. 12000–12010, 2019.

[21] H. Guillet de Chatellus, L. R. Cortés, and J. Azaña, "Optical real-time Fourier transformation with kilohertz resolutions," Optica, vol. 3, no. 1, pp. 1–7, 2016.

[22] C. Schnébelin and H. Guillet de Chatellus, "Agile photonic fractional Fourier transformation of optical and RF signals," Optica, vol. 4, no. 8, pp. 907–910, 2017.

[23] V. Durán, C. Schnébelin, and H. Guillet de Chatellus, "Coherent multi-heterodyne spectroscopy using acousto-optic frequency combs," Opt. Express, vol. 26, no. 11, pp. 13800–13809, 2018.

[24] G. Agrawal, Applications of Nonlinear Fiber Optics. Academic, Inc., 2008.

[25] V. Duran, L. Djevarhidjian, and H. Guillet de Chatellus, "Bidirectional frequency-shifting loop for dual-comb spectroscopy," Opt. Lett., vol. 44, no. 15, pp. 3789–3792, 2019.

[26] J. Azaña and M. A. Muriel, "Temporal self-imaging effects: theory and application for multiplying pulse repetition rates," IEEE J. Sel. Top. Quantum Electron., vol. 7, pp- 728–744, 2001.

[27] L. Romero-Cortés, H. Guillet de Chatellus, and J. Azaña, "On the generality of the Talbot condition for inducing self imaging effects on periodic objects," Opt. Lett. vol. 41, pp. 340–343, 2016. Erratum, Opt. Lett. vol. 41, p. 5748, 2016.

[28] C. R. Fernández-Pousa, "On the structure of quadratic Gauss sums in the Talbot effect," J. Opt. Soc. Am. A vol. 34, pp. 732–742, 2017.

[29] H. Guillet de Chatellus et al., "Generation of ultrahigh and tunable repetition rates in CW injection-seeded frequency-shifted feedback lasers," Opt. Express, vol. 21, no. 13, pp. 15065–15074, 2013.

[30] C. Schnébelin, and H. Guillet de Chatellus, "Optical spectral shaping with MHz resolution for arbitrary RF waveform generation," Conference on Lasers and Electro-Optics (CLEO), San Jose, CA, 2018, pp. 1-2.